PAPER

Robust superhydrophobic and self-lubricating PTES-TiO$_2$@UHMWPE fabric and its tribological properties†

Deke Li[ac] and Zhiguang Guo[*ab]

A superhydrophobic/self-lubricating fabric with double hierarchical structure was prepared by first etching pristine ultrahigh molecular weight polyethylene (UHMWPE) fibers with air-plasma, followed by a facile *in situ* growth method. Scanning electron microscopy (SEM) showed that the air-plasma etching treatment generated pits on the fiber surface and TiO$_2$ was grafted onto the etched fiber, which greatly improved its surface roughness. The fabric was further modified by 1H,1H,2H,2H-perfluorodecyltriethoxysilane (PTES), which possesses a low surface free energy. The results showed the PTES-TiO$_2$@UHMWPE fabric possessed superhydrophobic properties with a water contact angle (WCA) of 157.75°, enhanced thermal resistance, and exhibited excellent antiwear properties with a friction coefficient of 0.05. In addition, the PTES-TiO$_2$@UHMWPE fabric retained its superhydrophobicity without an apparent reduction after 30 cycles of washing or 5 minutes of friction treatment, revealing its good mechanical properties. Meanwhile, the mechanical strength of the fabric had little reduction after UV irradiation, which is helpful in enlarging the fabric applications in industry.

1. Introduction

Fabrics have been applied in electronics, medical and aerospace industries in the past decades due to their excellent properties, such as flame retardancy, conductivity, antibacterial, flame resistance, self-cleaning and wear resistance.[1–6] With the development of the research of functional fabrics, woven fabrics have been employed to fabricate hydrophobic fabrics as flexible substrates. The pristine ultrahigh molecular weight polyethylene (UHMWPE) fabrics are one of the most desirable high-performance woven fabrics owing to their high modulus, high axial tensile strength, self-lubricating properties, softness, low specific weight, high impact resistance, excellent chemical resistance and low dielectric constant.[7,8] However, the pristine UHMWPE fabric is easily wetted by water, since there are lots of hydrophilic groups on the surface of pristine UHMWPE fabrics. In addition, pristine UHMWPE fabrics show inherent drawbacks, such as weak thermal stability, chemical inertness, and poor UV protection capability, which limit their applications to some extent.[9–11] Therefore, it is significant if pristine UHMWPE fabric was accompanied with

superhydrophobic properties. Based on it, they can be used as functional materials, such as self-lubricating fabric, oil–water separation fabric under the demanding conditions.

Until now, many physical and chemical methods have been employed to overcome the fabric defects, and many studies have been made to explore the wetting mechanism of fabric and fabricate superhydrophobic fabric. When the roll-off angle is less than 10° and the water contact angle (WCA) is more than 150°, the surface is considered as having superhydrophobic property. It is well known that the roughness surface and low surface free energy are two essential conditions for superhydrophobicity.[12–15] In order to obtain superhydrophobic fabric and improve adhesive strength, several modification treatments are adopted to enhance the surface roughness of fabric. Some strategies of surface treatment have been adopted to improve the surface roughness of fabric, including gas plasma, γ-radiation, corona discharge, alkali etching, and chemical modification.[16–22]

Besides that, various inorganic nanoparticles such as TiO$_2$, ZnO, silica, carbon nanotubes (CNTs), and grapheme have been successfully coated on fiber surface, by which the surface roughness can be improved effectively.[23–25] Liu *et al.* proposed a strategy to fabricate water-repellent cotton fabrics modified with CNTs, *via* the facile dip coating process. Moreover, the tribological and mechanical properties of fabric can be improved by filling some nanoparticles.[26] Zhang *et al.* investigated the tribological property and corresponding mechanical strength of the PTFE/Nomex fabric composites filled with MoSi$_2$.[27]

ᵃState Key Laboratory of Solid Lubrication, Lanzhou Institute of Chemical Physics, Chinese Academy of Sciences, Lanzhou 730000, People's Republic of China. E-mail: zguo@licp.cas.cn; Fax: +86-931-8277088; Tel: +86-931-4968105

ᵇHubei Collaborative Innovation Centre for Advanced Organic Chemical Materials, Ministry of Education Key Laboratory for the Green Preparation and Application of Functional Materials, Hubei University, Wuhan 430062, People's Republic of China

*ᶜUniversity of Chinese Academy of Sciences, Beijing 100049, People's Republic of China*

† Electronic supplementary information (ESI) available. See DOI: 10.1039/c6ra28255e

Among these nanoparticles of the inorganic metal oxides, TiO_2 has many special features that can be beneficial to achieve the multifunctional materials. For example, TiO_2 nanoparticles deposited on the fabric surface can improve its UV resistance and develop application field as reinforcements, corrosion resistant, self-cleaning fabrics, or other desired applications.[28] And more importantly, a rough surface for superhydrophobicity can be achieved from TiO_2 coatings, meanwhile, self-lubricating film of TiO_2 can also play an important role in resisting wear.[29] Therefore, TiO_2 nanoparticles can be selected as a suitable material for fabricating hydrophobic and antiwear PTES-TiO_2@UHMWPE fabrics. Many technical approaches have been adopted to prepare special property superhydrophobic fabric, such as chemical vapor deposition (CVD), dip-coating, spray-coating, polymerization and sol–gel.[30–35] However, the methods mentioned above are still the complicated technology to prepare superhydrophobic fabrics, and its shortcoming is that the adhesive strength is poor, so that the nanoparticle layer only weakly adheres to the surfaces of matrix, which is a barrier for its final application. At this point, the *in situ* growth technology possesses its own superiority. Superhydrophobic fabrics which are modified by inorganic nanoparticles *via* an *in situ* growth process which is a simple preparation technology without complicated equipment and exhibit excellent adhesive strength and robust mechanical property.[36]

Based on these studies, in this paper pristine UHMWPE fabric is treated by air-plasma, which can not only improve the cohesive action between the nanoparticle and the fabric, but also surface roughness is greatly enhanced. Moreover, TiO_2 nanoparticles were grafted on the fabrics with *in situ* growth method, as shown in Scheme 1.

Therefore, a simple way to fabricate superhydrophobic fabric by developing a dualscale roughness structure, and then modified by a fluorinated alkylsilane with low surface energy. Moreover, as-prepared fabrics realized filtration oils from water effectively, and can be reused many times. The obtained superhydrophobic fabric is robust, durable and antiwear. This work is expected that the facile method can be adopted to fabricate the versatile PTES-TiO_2@UHMWPE fabric for durable superhydrophobicity, efficient oil–water separation, stable thermal resistance, excellent wear resistance, and effective self-lubricating applications.
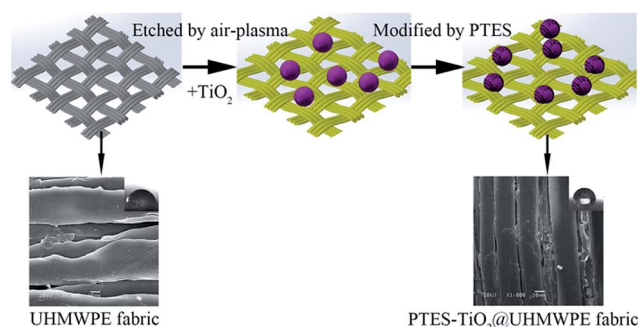
Scheme 1 Schematic diagram of the technological process for preparing hydrophobic and antiwear composite.

2. Experimental

2.1 Material

Pristine UHMWPE fabrics (weight: 180 g m^{-2}, fineness: 400 Denier, plain weave) were purchased from Dongguan sovetl special Rope & Webbing Co., Ltd., China. Potassium titanium oxalate (PTO) and 1H,1H,2H,2H-perfluorodecyltriethoxysilane (PTES) were obtained from Meryer (Shanghai) Chemical Technology Co., Ltd. and used as received. The other materials were analytically pure and used without further treatment.

2.2 Preparation of surface treated plasma-UHMWPE fabrics

The pristine UHMWPE fabric was purified with ethyl alcohol and petroleum ether in Soxhlet then washed with distilled water, finally dried in an oven at 60 °C. The pristine UHMWPE fabric surface was etched by air-plasma apparatus (Diener, Germany) with the power of 98 W for 10 min, and the prepared fabric was marked as plasma-UHMWPE fabric.

2.3 Fabrication of PTES-TiO_2@UHMWPE fabric

H_2O_2 (1 mL) was added into the deionized water solution (30 mL) containing an appropriate amount of PTO, and the mixed solution was stirred for 5 min at ambient temperature. Then the acid solution was dripped into the mixture solution to adjust the pH value to 1–2 by electromagnetic stirring. The plasma-UHMWPE fabric was soaked in the solution, followed by a facile one-pot hydrothermal reaction at 80 °C for 12 h to fabricate TiO_2 particle on plasma-UHMWPE fabrics. The fabric was cleaned with distilled water to wash away residues. The content of TiO_2 particles (W (%)) can be calculated by the following formula:

$$W = \frac{W_0 - W_1}{W_0} \times 100\%$$

where W_0 and W_1 are the weights of prepared fabric and plasma-UHMWPE fabric, respectively. Subsequently, the plasma-UHMWPE fabric was put into surface modifying agents, which was consisted of 1 vol% PTES in methanolic solution. Finally, the superhydrophobic PTES-TiO_2@UHMWPE fabric was fabricated by drying at 60 °C, and the samples of different TiO_2 contents were obtained according to preceding technology.[36]

2.4 Characterization of PTES-TiO_2@UHMWPE fabric

The samples morphology images were studied by a scanning electron microscopy (SEM, JSM-5600LV, Japan), and the samples were treated by Au-spraying before observation. X-ray photoelectron spectroscopy (XPS, ESCALAB 250Xi, Thermo Fisher Scientific) was employed to measure the elements using Al Kα X-ray source. The thermogravimetric (TG) analysis was examined by using a simultaneous thermal analyzer (STA, 449C, NETZSCH) measurement. The specimens were heated from 50 to 700 °C in nitrogen environment with heating velocity of 10 °C min^{-1}. Fourier transformer infrared (FTIR, Nexus 870, Nicolet) spectrometer was used to analyze the chemical structure of the samples. The WCA was measured by a JC2000D1CA meter (Shanghai Zhongchen Digtal Technology Apparatus Co., Ltd,

China) to evaluate the wettability of samples, and a 5 μL distilled water droplet was dripped on the different regions of the sample at ambient temperature.

The superhydrophobic durability and tribological property of PTES-TiO$_2$@UHMWPE were assessed by a MMQ-05G pin-on-disk tribometer (Jinan Yihua Tribology Testing Technology Co. Ltd, China) under dry friction condition, the principle diagram of the friction (see Fig. 1S, ESI†). The samples were fixed on a disk with rotational velocity of 286 rpm and the external load was 10 N. AISI-1045 round pin (diameter: Ø = 4.5 mm) was polished with 400, 800, and 1000 grade metallographic abrasive paper and washed with acetone before the test. When the pin was sliding against the disk, the friction coefficient was recorded by computer. The tensile strength was performed on a universal material testing machine (DWD-200) at a stretching velocity of 5 mm min^{-1} on the basis of the standard ISO527-2:1993. According to the tensile strength test standard, the size of the specimen was 100×20 (mm) and the thickness was measured. The tensile strength σ_b (MPa) is calculated by the following formula:

$$\sigma_b = F_p(BD)^{-1}$$

where F_p (N) is drawing force, B (m) and D (m) are width and thickness of the specimen, respectively. Each sample mentioned above was measured for three times to obtain the average value.

3. Results and discussion

3.1 Surface morphology analysis

The surface microstructure is essential for material with superhydrophobic property.[37] Based on the wetting models, air pockets can be trapped between solid and liquid surface of hierarchical structure. And the contact surface can be decreased when water droplet fell to the surface with hierarchical structure.[38] Therefore, the woven fiber grid of PTES-TiO$_2$@UHMWPE fabric is an ideal hierarchical structure for superhydrophobic

surface. SEM was employed to observe the surface morphology of pristine UHMWPE fabric, plasma-UHMWPE fabric and PTES-TiO$_2$@UHMWPE fabric, as shown in Fig. 1. The fiber surface of pristine UHMWPE fabric showed relatively smooth (see Fig. 1(a)).

After being etched by air-plasma at 98 W for 10 min, the fiber surface was full of tiny holes (see Fig. 1(b)). Therefore, the treatment of air-plasma is a good technique to attain the surface roughness of plasma-UHMWPE fabric. This coarse surface is more beneficial to fabricate superhydrophobicity, because air can be captured in the tiny holes. The PTES-TiO$_2$@UHMWPE fabric was modified by PTES with lower surface free energy, moreover, the composite had microscopic roughness on the fiber surface (see Fig. 1(c)). These special surface morphology and structure play an important role in preparation of superhydrophobic surface.

3.2 Characterization

FTIR spectroscopy of the pristine-UHMWPE fabric and PTES-TiO$_2$@UHMWPE fabric are observed from Fig. 2. PTES-TiO$_2$@UHMWPE fabric presented absorption bands at around 1087 and 820 cm^{-1} when compared with the pristine UHMWPE fabric. It can be the stretching vibrations of Si–O–C and Si–C, respectively. The peaks were found at around 1360–1124 cm^{-1}, which can be assigned to the groups of –CF$_2$ and –CF$_3$. Moreover, Ti–OH and Ti–O groups were detected at around 2500–3700 cm^{-1} and 890 cm^{-1}, respectively. Therefore, it is reasonable to infer that the pristine UHMWPE fabric surface was effectively modified by TiO$_2$ nanoparticles and PTES.[39–41]

In addition, the samples were further analyzed by X-ray photoelectron spectroscopy (XPS), and the surface composition of the PTES-TiO$_2$@UHMWPE fabric was investigated, as shown in Fig. 3. The peaks of C and O were detected at the corresponding position for the pristine UHMWPE fabric (Fig. 3(a)). Therefore, the pristine UHMWPE fabric was
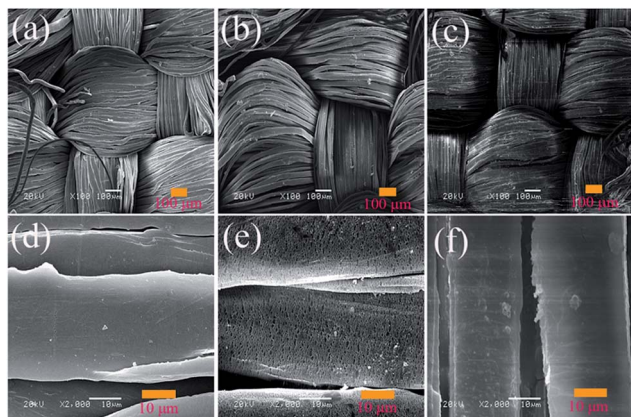

Fig. 1 SEM images of pristine UHMWPE fabric (a), plasma-UHMWPE fabric (b) and PTES-TiO$_2$@UHMWPE fabric (c), (d)–(f) are magnified images of (a)–(c), respectively.
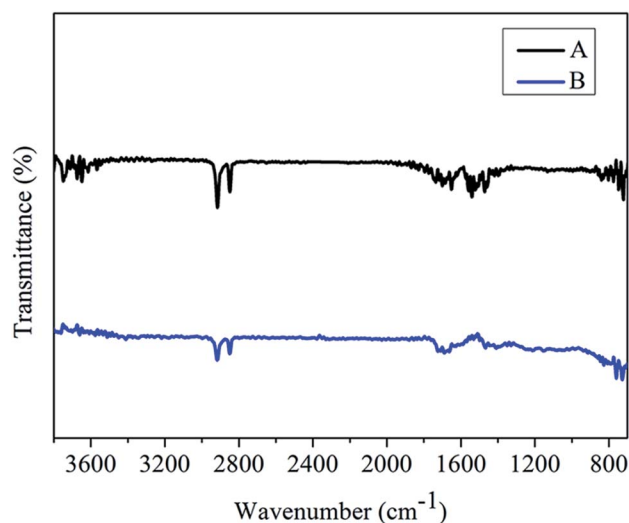

Fig. 2 FTIR spectroscopy of the pristine UHMWPE fabric (denoted as (A)) and PTES-TiO$_2$@UHMWPE fabric (denoted as (B)).
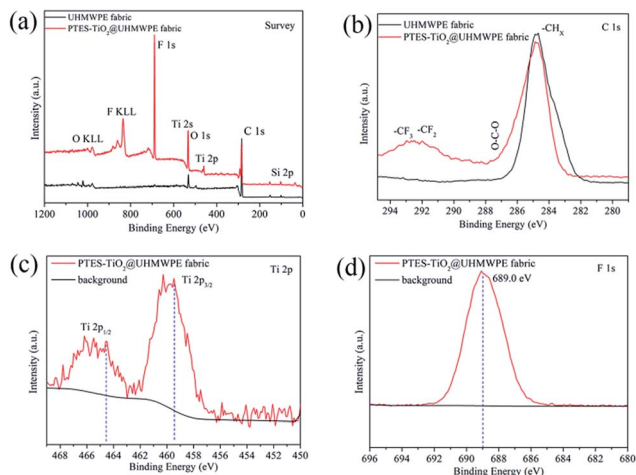
Fig. 3 XPS spectra of the pristine UHMWPE fabric and PTES-TiO$_2$@ UHMWPE fabrics (a), corresponding high-resolution XPS spectra of C 1s (b), Ti 2p (c) and F 1s (d).

composed of the carbon, oxygen and some other element. However, the peaks which correspond Ti 2p and F 1s were detected in the XPS survey spectra of the PTES-TiO$_2$@UHMWPE fabric, together with the –CF$_2$, –CF$_3$, –CH$_X$, O–C–O, C–O peaks, which indicated that the UHWPE fabric surface had been modified by TiO$_2$ particles and PTES (Fig. 3(a)). The high resolution C 1s peak were resolved into peaks of 288.1, 286.6, and 285.0, which can be O–C–O, C–H, and C–C molecular bonds, respectively (Fig. 3(b)). Ti 2p was observed at 458.9 and 464.6 eV, which can be assigned to Ti 2p$_{3/2}$ and 2p$_{1/2}$, respectively (Fig. 3(c)). The F 1s peak was detected at 689.0 eV (Fig. 3(d)), and the peaks at 291.8 and 294.1 eV were assigned to –CF$_2$ and –CF$_3$, respectively (Fig. 3(b)).[42]

3.3 Thermal properties

The thermostability of samples can be analyzed by thermogravimetric (TG) analysis under N$_2$ atmosphere.[43] The TG and DTG curves of the pristine UHMWPE fabric and PTES-TiO$_2$@ UHMWPE fabric are shown in Fig. 4, and the values of the temperature of the initial decomposition (T_{di}), the maximum degradation rate temperature (T_{max}) and carbon yield (Y_c) at 800 °C can be obtained from the curves. The values of T_{di}, T_{max} and Y_c indicate that the samples had different mechanisms of thermal decomposition. The T_{di} value of the PTES-
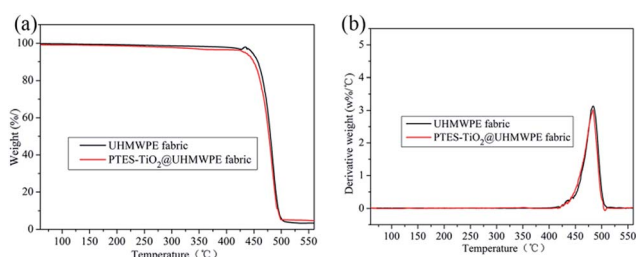
TiO$_2$@UHMWPE fabric was smaller than of the pristine fabric, the reason for it can be dyed to the weak heat endurance of the graft chain. However, the peak strength of the PTES-TiO$_2$@ UHMWPE fabric was lower, by PTES and TiO$_2$, probably indicating that thermal decomposition is hindered after being modified by PTES and TiO$_2$. Meanwhile, the values of T_{max} and Y_c were higher comparing to that of the pristine fabric, which suggests that the thermostability of the PTES-TiO$_2$@UHMWPE fabric can be improved with surface treated with PTES and TiO$_2$. In the process of thermal decomposition, inner inorganic layers of titania and silica can be generated from TiO$_2$ and PTES, which can prevent degradation of the PTES-TiO$_2$@UHMWPE fabric as a thermal barrier.[44] On the other hand, with the photooxidation action of the incorporation of TiO$_2$ and PTES, the dehydrogenation reaction can be accelerated between the PTES-TiO$_2$@UHMWPE molecular chains and Y_c be increased accordingly. In summary, thermal stability of PTES-TiO$_2$@ UHMWPE fabric was more stable to some extent.

3.4 Surface wettability

The wettability of the pristine UHMWPE fabric and the PTES-TiO$_2$@UHMWPE fabric was shown in Fig. 5. When water droplets (5 µL) were dropped onto the samples, the pristine UHMWPE fabric is wetted. The contact angle (CA) was lower than 90° to water, suggesting that the pristine UHMWPE fabric was superhydrophilic. It can be due to the capillary action of the fiber and porosities of woven fibrous structure. When the pristine UHMWPE fabric was modified by the PTES and TiO$_2$, the fabric surface formed sphere-like water droplets with CA of 157° and the droplets did not infiltrate into the fiber immediately. The surface roughness is an essential condition for superhydrophobicity of fabric.[45] The hierarchically dual-scale surface structure was formed from etched fabrics, and the air was trapped between the solid–liquid interface. On the other hand, fluoromethyl groups were packed on the fiber surface. Therefore, the superhydrophobicity of the PTES-TiO$_2$@UHMWPE
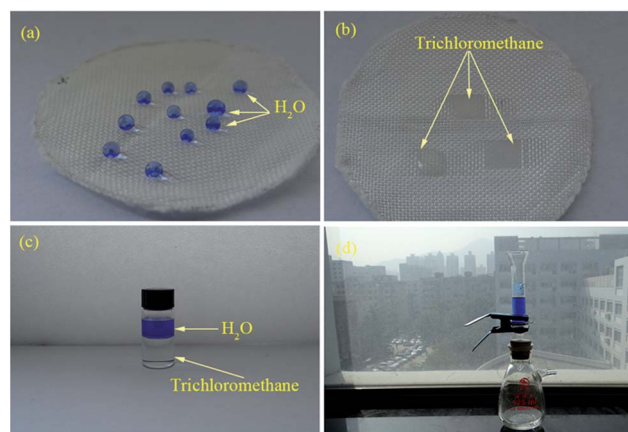

Fig. 5 Water on the surface of the PTES-TiO$_2$@UHMWPE fabrics (a); oil on the surface of the PTES-TiO$_2$@UHMWPE fabrics (b); and oil–water separation process (d) and the water was dyed with methylene blue for discrimination (c).

Fig. 4 The TG and DTG analyses of the pristine UHMWPE fabric and PTES-TiO$_2$@UHMWPE fabrics.

fabric is a result of the combined effect between the rougher surfaces and the low surface energy PTES grafted on the pristine UHMPE fabric surface.

As shown in Fig. 5, the superhydrophobic PTES-TiO₂@ UHMWPE fabric are oleophilic, and the obtained fabric can be tested by an oil–water separation experiment.[46,47] When the mixtures of trichloromethane and methylene blue dyed water were poured onto the PTES-TiO₂@UHMWPE fabric, the oil could penetrate through the fabric separately, but methylene blue dyed water remained on the fabric surface. This indicates that the PTES-TiO₂@UHMWPE fabric can separate oil–water mixtures with special surface wettability (Fig. 5(c)). In addition, the PTES-TiO₂@UHMWPE fabric can still keep the capacity for oil–water separation after several experiments.

3.5 Superhydrophobic fabric durability and tribological property

The hydrophobic property of PTES-TiO₂@UHMWPE fabric contained TiO₂ coating can been influenced by increasing the content of the PTO, the fabric modified by 0.80 mM PTO exhibit the WCA of about 157° (Fig. 6(a)). Concerning in practical applications, it is necessary to evaluate the washing durability and the abrasive resistance of the superhydrophobic fabric.[48] The mechanical durability of the superhydrophobic surface was investigated by a friction test, the schematic of the friction for fabrics as mentioned above. From the image of the WCA and the abrasion time for the PTES-TiO₂@UHMWPE (0.80 mM) (Fig. 6(b)), the WCA decreased with friction time prolonging and the WCA of PTES-TiO₂@UHMWPE (0.80 mM) becomes less than 110° after 10 minutes. This decrease of superhydrophobicity might be due to the partial removing of the surface roughness and the loss of the layer of PTES and TiO₂ during friction process. The excellent mechanical wear resistance of the PTES-TiO₂@UHMWPE fabrics might be provided by lubricant of PTES and TiO₂, and self-lubricant fabric which has not only good wear
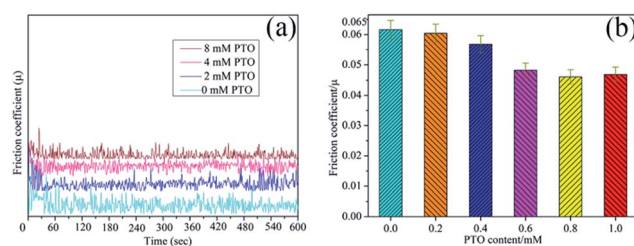

Fig. 7 Friction curve (a) and friction coefficient (b) of PTES-TiO₂@ UHMWPE fabric with the content of PTO.

resistance but also a strong adhesive force to fibers after air-plasma treatment.

Moreover, the laundering durability of the super-hydrophobic surface is evaluated by a American Association of Textile Chemists and Colorists 61-2006 modified methods. The variation trend of the WCA with different washing cycles is shown in Fig. 6(c). The WCA of PTES-TiO₂@UHMWPE fabric (PTO = 0.80 mM) was about 158.05° before the washing test, and then the WCA gradually decreased with the increasing of washing cycles. This is because that the roughness of the modified fiber surface was partially washed away. However, the result shows that the WCA was about 149.95° without much change and the water droplets remained spherical after 30 cycles of laundering, as shown in Fig. 6(c), which may be due to the intrinsic surface roughness of the fiber was exposed during the washing process. This indicates that the PTES-TiO₂@ UHMWPE fabrics have better stability for superhydrophobicity under water shear forces.[49] These results indicate that the modified layer was adhered to the PTES-TiO₂@UHMWPE fabric surfaces and hydrophobicity was still remained even after several washing cycles and continual abrasion.

The tribological property of fabric was tested under the dry sliding conditions, the friction coefficient was obtained from computer directly, as shown in Fig. 7. The friction is decreased slightly with the PTO content increasing. The PTES-TiO₂@ UHMWPE fabric modified with PTO (0.80 mM) shows the lowest friction coefficient with value of 0.05, and the friction curve is more stable. Therefore, the modifier of PTES and TiO₂ can improve the antifriction property of pristine UHMWPE fabric. Then abrasion is aggravated with the PFTS-TiO₂ content further increase, and the friction coefficient can be reached to above 0.05 with the wave friction curves.

The abrasion resistance is the synergistic action of self-lubricant pristine UHMWPE fabric and modifier content. The TiO₂ nanoparticles were grafted uniformly onto fabric by *in situ* growth and the adhesive property was enhanced after plasma, which prevented stress concentration to alleviate external force. Sliding contact of friction interface is turned into rolling contact that effectively avoids direct contact between worn surface and friction pin. When the PTES-TiO₂@UHMWPE fabric is modified with PTO more than 0.80 mM, the wear resistance is worse due to the reduction of the interfacial strength of fabric and modifier matrix. And the friction behavior of the composite is influenced by the abrasive particles of cut fibers and TiO₂ which
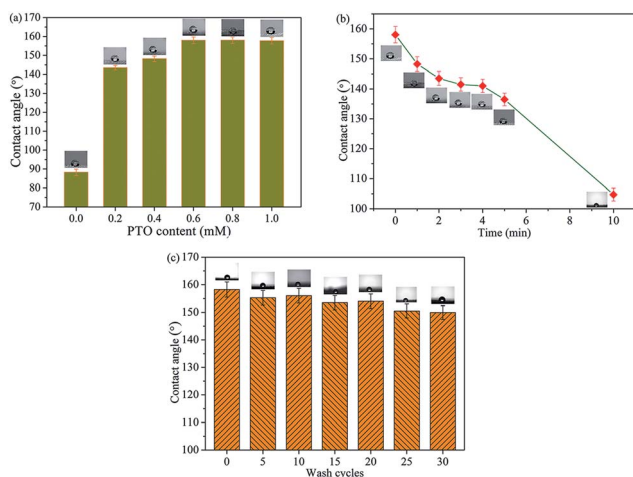

Fig. 6 The WCA of PTES-TiO₂@UHMWPE fabric with the content of PTO (a), the variation WCA of PTES-TiO₂@UHMWPE fabric (PTO = 0.80 mM) with abrasion time (b) and the number of wash cycles (c).
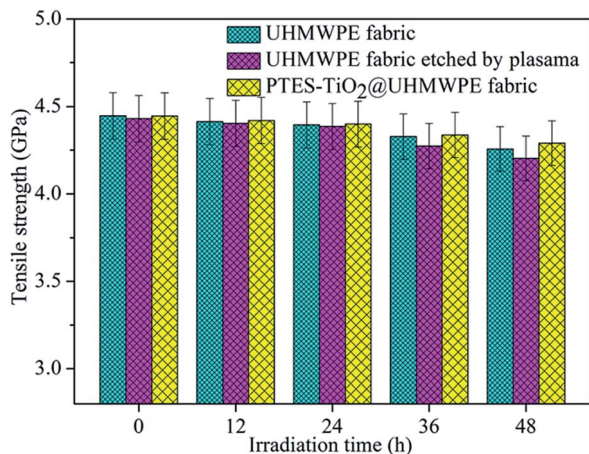
Fig. 8 Tensile strength of pristine UHMWPE fabric, plasma-UHMWPE fabric and PTES-TiO$_2$@UHMWPE fabric.

are formed in the friction process. Therefore, the appropriate content TiO$_2$ modifier can improve the wear resistance of pristine UHMWPE fabric.

3.6 Mechanical properties

Mechanical strength is a critical parameter for superhydrophobic PTES-TiO$_2$@UHMWPE fabric, which can ensure that PTES-TiO$_2$@UHMWPE fabrics can not be destroyed in the practical application for a long time. Tensile strength of pristine UHMWPE fabric, plasma-UHMWPE fabric and PTES-TiO$_2$@ UHMWPE fabric are shown in Fig. 8. Tensile strength of the pristine UHMWPE fabric is 4.45 GPa. After treating with air-plasma, the tensile strength decreases to about 4.43 GPa, which is caused by degradation of air-plasma treatment, and then the molecular chains of plasma-UHMWPE fibers are dislocated in the tensile process. After modified by PTES and TiO$_2$, the tensile strength of PTES-TiO$_2$@UHMWPE fabric can increase to about 4.45 GPa. The reason is that stress is more evenly distributed between the PTES-TiO$_2$@UHMWPE fibers under the condition of stretching, and the stress concentration is reduced after modification because the grafted layer attached to the fabric is an elastomer. Moreover, the crosslinked layers are formed on the surface of PTES-TiO$_2$@UHMWPE fiber, which is composed of the chemical bonds of Si–O, Ti–O, and Si–O–Ti. The crosslinked structure prevents the chains from slipping with the presence of external force.

The samples were irradiated by UV exposure with different time at room temperature, and strength was decreased differently with the increase of UV exposure time, as shown in Fig. 8. For the pristine UHMWPE, plasma-UHMWPE and PTES-TiO$_2$@ UHMWPE fibers, the magnitudes of the break strength are 4.27%, 5.12%, and 3.49% after the UV irradiation, respectively. The mechanical properties of pristine UHMWPE fabric and the air-plasma fabric are rapidly decreased after 48 h of irradiation, which can be attributed to rupture of the fiber molecular chains and dehydrogenation. The mechanical properties of PTES-TiO$_2$@UHMWPE modified with PTES and TiO$_2$ is slightly better

than of the pristine UHMWPE fiber. With regard to PTES-TiO$_2$@UHMWPE, TiO$_2$ has better UV absorption capacity, and interlaced structures of Si–O–Si group are grafted on the PTES-TiO$_2$@UHMWPE fiber surface, which can prevent PTES-TiO$_2$@UHMWPE fiber from rapid degradation in the course of tension.

4. Conclusion

In this study, we have demonstrated a simple approach for TiO$_2$ nanoparticles deposition on pristine UHMWPE fabric surface by hydrothermal reaction. And durable superhydrophobic surface of PTES-TiO$_2$@UHMWPE were prepared with modification in PTES solution. The PTES-TiO$_2$@UHMWPE fabrics exhibited excellent hydrophobicity, oil–water separation capability and laundering durability, compared with those of the pristine UHMWPE fabric showed excellent mechanical stability and antiwear property. In addition, this facile approach for fabricating durable superhydrophobic fabrics can avoid the use of complex equipment and be easily applied to other fabrics substrates for scale production. Furthermore, these robust superhydrophobic PTES-TiO$_2$@UHMWPE fabrics can be applied in various fields including UV protection, self-lubrication and oil–water separation.

Acknowledgements

References

1 D. Yu, G. Kang, W. Tian, L. Lin and W. Wang, *Appl. Surf. Sci.*, 2015, **357**, 1157–1162.

2 C. H. Xue, L. Zhang, P. B. Wei and S. T. Jia, *Cellulose*, 2016, **23**, 1471–1480.

3 A. Nazari, M. Montazer and M. Dehghani-Zahedani, *Ind. Eng. Chem. Res.*, 2013, **52**, 1365–1371.

4 C. H. Xue, X. Li, S. T. Jia, X. J. Guo and M. Li, *RSC Adv.*, 2016, **6**, 84887–84892.

5 X. L. Zhu, L. Yuan, G. Z. Liang and A. J. Gu, *J. Mater. Chem. A*, 2015, **3**, 12515–12529.

6 C. Tan, Q. Li, Y. M. Li, C. Q. Zhang and L. Xu, *RSC Adv.*, 2016, **6**, 53813–53820.

7 M. Shateri-Khalilabad and M. E. Yazdanshenas, *Cellulose*, 2013, **20**, 3039–3051.

8 F. X. Chen, H. Y. Yang, X. Liu, D. Z. Chen, X. F. Xiao, K. S. Liu, J. Li, F. Cheng, B. H. Dong, Y. S. Zhou, Z. G. Guo, Y. Qin, S. M. Wang and W. L. Xu, *ACS Appl. Mater. Interfaces*, 2016, **8**, 5653–5660.

9 H. Zhang, M. Shi, J. Zhang and S. Wang, *J. Appl. Polym. Sci.*, 2003, **89**, 2757–2763.

10 S. P. Lin, J. L. Han, J. T. Yeh, F. C. Chang and K. H. Hsieh, *Eur. Polym. J.*, 2007, **43**, 996–1008.

11 J. T. Hu, Q. H. Gao, L. Xu, M. X. Zhang, Z. Xing, X. J. Guo, K. Zhang and G. Z. Wu, *ACS Appl. Mater. Interfaces*, 2016, **8**, 23311–23320.

12 B. Wang, W. X. Liang, Z. G. Guo and W. M. Liu, *Chem. Soc. Rev.*, 2015, **44**, 336–361.

13 Y. Hou, Z. Wang, J. Guo, H. Shen, H. Zhang, N. Zhao, Y. Zhao, L. Chen, S. Liang, Y. Jin and J. Xu, *J. Mater. Chem. A*, 2015, **3**, 23252–23260.

14 I. K. Oh, K. Kim, Z. Lee, K. Y. Ko, C. W. Lee, S. J. Lee, J. M. Myung, C. Lansalot-Matras, W. Noh, C. Dussarrat, H. Kim and H. B. R. Lee, *Chem. Mater.*, 2015, **27**, 148–156.

15 E. Bittoun and A. Marmur, *Langmuir*, 2012, **28**, 13933–13942.

16 G. Y. Bae, B. G. Min, Y. G. Jeong, S. C. Lee, J. H. Jang and G. H. Koo, *J. Colloid Interface Sci.*, 2009, **337**, 170–175.

17 Z. Z. Zhang, B. Ge, X. H. Men and Y. Li, *Colloids Surf., A*, 2016, **490**, 182–188.

18 C. X. Wang, M. Du, J. C. Lv, Q. Q. Zhou, D. W. Gao, G. L. Liu, L. M. Jin, Y. Ren and J. H. Liu, *Fibers Polym.*, 2015, **16**, 333–342.

19 T. T. Hanh, P. D. Van, N. T. Thu, L. Quoc, D. N. B. Duyen and N. Q. Hien, *Carbohydr. Polym.*, 2014, **101**, 1243–1248.

20 W. Xu and X. Liu, *Eur. Polym. J.*, 2003, **39**, 199–202.

21 C. L. Zhang, P. Li and B. Cao, *Ind. Eng. Chem. Res.*, 2016, **55**, 5030–5035.

22 L. H. Peng, R. H. Guo, J. W. Lan, S. X. Jiang and S. J. Lin, *Appl. Surf. Sci.*, 2016, **386**, 151–159.

23 Q. H. Gao, J. T. Hua, R. Li, L. J. Pang, Z. Xing, L. Xua, M. H. Wang, X. J. Guo and G. Z. Wu, *Carbohydr. Polym.*, 2016, **149**, 308–316.

24 H. Zhou, H. X. Wang, H. T. Niu, A. Gestos and T. Lin, *Adv. Funct. Mater.*, 2013, **23**, 1664–1670.

25 B. Wang, J. Li, G. Y. Wang, W. X. Liang, Y. B. Zhang, L. Shi, Z. G. Guo and W. M. Liu, *ACS Appl. Mater. Interfaces*, 2013, **5**, 1827–1839.

26 Y. Y. Liu, X. W. Wang, K. H. Qi and J. H. Xin, *J. Mater. Chem.*, 2008, **18**, 3454–3460.

27 G. N. Ren, Z. Z. Zhang, X. T. Zhu, M. M. Yang, X. H. Men, W. Jiang and W. M. Liu, *Compos. Sci. Technol.*, 2014, **104**, 146–151.

28 E. Pakdel, W. A. Daud and X. Wang, *Text. Res. J.*, 2015, **85**, 1404–1428.

29 X. W. Qi, Z. N. Jia and Y. L. Yang, *J. Appl. Polym. Sci.*, 2013, **130**, 2100–2105.

30 I. S. Bayer, D. Fragouli, A. Attanasio, B. Sorce, G. Bertoni, R. Brescia, R. D. Corato, T. Pellegrino, M. Kalyva, S. Sabella, P. P. Pompat, R. Cingolani and A. Athanassiou, *ACS Appl. Mater. Interfaces*, 2011, **3**, 4024–4031.

31 H. Teisala, M. Tuominen, M. Aromaa, M. Stepien, J. M. Makela, J. J. Saarinen, M. Toivakka and J. Kuusipalo, *Langmuir*, 2012, **28**, 3138–3145.

32 D. Nystrom, J. Lindqvist, E. Ostmark, A. Hult and E. Malmstrom, *Chem. Commun.*, 2006, **34**, 3594–3596.

33 Y. C. Sheen, W. H. Chang, W. C. Chen, Y. H. Chang, Y. C. Huang and F. C. Chang, *Mater. Chem. Phys.*, 2009, **114**, 63–68.

34 A. Berendjchi, R. Khajavi and M. E. Yazdanshenas, *Nanoscale Res. Lett.*, 2011, **6**, 594–601.

35 H. Jin, M. Kettunen, A. Laiho, H. Pynnönen, J. Paltakari, A. Marmur, O. Ikkala and R. H. A. Ras, *Langmuir*, 2011, **27**, 1930–1934.

36 J. Y. Huang, S. H. Li, M. Z. Ge, L. N. Wang, T. L. Xing, G. Q. Chen, X. F. Liu, S. S. Al-Deyab, K. Q. Zhang, T. Chen and Y. K. Lai, *J. Mater. Chem. A*, 2015, **3**, 2825–2832.

37 B. Wang, Y. B. Zhang, L. Shi, J. Li and Z. G. Guo, *J. Mater. Chem.*, 2012, **22**, 20112–20127.

38 R. N. Wenzel, *Ind. Eng. Chem.*, 1936, **28**, 988–994.

39 S. Vives and C. Meunier, *Ceram. Int.*, 2008, **34**, 37–44.

40 D. B. Mahadik, A. V. Rao, A. P. Rao, P. B. Wagh, S. V. Ingale and S. C. Gupta, *J. Colloid Interface Sci.*, 2011, **356**, 298–302.

41 K. Jeyasubramanian, G. S. Hikku, A. V. M. Preethi, V. S. Benitha and N. Selvakumar, *J. Ind. Eng. Chem.*, 2016, **37**, 180–189.

42 Y. K. Lai, Y. X. Tang, J. J. Gong, D. G. Gong, L. F. Chi, C. J. Lin and Z. Chen, *J. Mater. Chem.*, 2012, **22**, 7420–7426.

43 Y. W. Gao, A. J. Gu, Y. C. Jiao, Y. L. Yang, G. Z. Liang, J. T. Hu, W. Yao and L. Yuan, *Polym. Adv. Technol.*, 2012, **23**, 919–928.

44 X. L. Zhu, L. Yuan, G. Z. Liang and A. J. Gu, *J. Mater. Chem. A*, 2015, **3**, 12515–12529.

45 S. T. Wang, L. Feng and L. Jiang, *Adv. Mater.*, 2006, **18**, 767–770.

46 Z. Y. Deng, W. Wang, L. H. Mao, C. F. Wang and S. Chen, *J. Mater. Chem. A*, 2014, **2**, 4178–4184.

47 Z. L. Xu, K. Miyazaki and T. Hori, *Appl. Surf. Sci.*, 2016, **370**, 243–251.

48 M. Wu, B. Ma, T. Pan, S. Chen and J. Sun, *Adv. Funct. Mater.*, 2016, **26**, 569–576.

49 B. Deng, R. Cai, Y. Yu, H. Q. Jiang, C. L. Wang, J. Li, L. F. Li, M. Yu, J. Y. Li, L. D. Xie, Q. Huang and C. H. Fan, *Adv. Mater.*, 2010, **22**, 5473–5477.